
Penalty Method for Inversion-Free Deep Bilevel Optimization

Akshay Mehra¹ Jihun Hamm¹

Abstract

Bilevel optimizations are at the center of several important machine learning problems such as hyperparameter tuning, data denoising, few-shot learning, data poisoning. Different from simultaneous or multi-objective optimization, obtaining the exact descent direction for continuous bilevel optimization requires computing the inverse of the hessian of the lower-level cost function, even for first order methods. In this paper, we propose a new method for solving bilevel optimization, using the penalty function, which avoids computing the inverse of the hessian. We prove convergence of the method under mild conditions and show that it computes the exact hypergradient asymptotically. Small space and time complexity of our method allows us to solve large-scale bilevel optimization problems involving deep neural networks with up to 3.8M upper-level and 1.4M lower-level variables. We present results of our method for data denoising on MNIST/CIFAR10/SVHN datasets, for few-shot learning on Omniglot/Mini-Imagenet datasets and for training-data poisoning on MNIST/Imagenet datasets. In all experiments, our method outperforms or is comparable to previously proposed methods both in terms of accuracy and run-time.

1. Introduction

Bilevel optimizations appear in many fields of study where there are two competing parties or objectives involved. Particularly, a bilevel problem arises, if one party makes its choice first affecting the optimal choice of the second party, also known as the Stackelberg model, dating back to 1930’s [33]. The general form of a bilevel optimization problem is

$$\min_u f(u, v), \quad \text{s.t.} \quad v = \arg \min_v g(u, v). \quad (1)$$

¹Department of Computer Science, Tulane University. Correspondence to: Akshay Mehra <amehra@tulane.edu>, Jihun Hamm <jhamm3@tulane.edu>.

A bilevel problem with constraints is of the form $\min_{u \in \mathcal{U}} f(u, v)$, s.t. $v = \arg \min_{v \in \mathcal{V}(u)} g(u, v)$, where the lower-level constraint set $\mathcal{V}(u)$ can depend on u . However, we focus on unconstrained problems in this paper. The ‘upper-level’ problem $\min_u f(u, v)$ is a usual minimization problem except that v is constrained to be the solution to the ‘lower-level’ problem $\min_v g(u, v)$ which is dependent on u (see [3] for a review of bilevel optimization). Bilevel optimizations also appears in many important machine learning problems. For example, gradient-based hyperparameter tuning [8; 19; 17; 25; 10; 11], data denoising by importance learning [16; 34; 27], few-shot learning [26; 28; 32; 10; 21; 31; 11], and training-data poisoning [19; 22; 14; 30]. We explain each of these problems and their bilevel formulations below.

Gradient-based hyperparameter tuning. Finding hyperparameters is an indispensable step in any machine learning problem. Grid search is a popular way of finding the optimal hyperparameters, if the domain of the hyperparameters is a predetermined discrete set or a range. However, when losses are differentiable functions of the hyperparameter(s), we can find optimal hyperparameter values by solving a continuous bilevel optimization. Let u and w denote hyperparameter(s) and parameter(s) for a class of learning algorithms and $h(x; u, w)$ be the hypothesis. Then $L_{\text{val}}(u, w) := \frac{1}{N_{\text{val}}} \sum_{(x_i, y_i) \in \mathcal{D}_{\text{val}}} l(h(x_i; u, w), y_i)$ is the validation loss, and $L_{\text{train}}(u, w)$ is the training loss, defined similarly. The best hyperparameter(s) u is then the solution to the following problem

$$\min_u L_{\text{val}}(u, w) \quad \text{s.t.} \quad w = \arg \min_w L_{\text{train}}(u, w). \quad (2)$$

Thus, we find the best model parameters w for each choice of the hyperparameter u , and select that value for the hyperparameter u which incurs the smallest validation loss.

Data denoising by importance learning. A common assumption of learning is that the training examples are i.i.d. samples from the same distribution as the test data. However, if training and testing distributions are not identical or if the training examples have been corrupted by noise or modified by adversaries, this assumption is violated. In such cases, re-weighting the importance of each training example, before training, can help reduce the discrepancy between the two distributions. For example, one can up-weight the importance of the examples from the same

distribution and down-weight the importance of the rest. This problem of finding the correct weight for each training example can be formulated as a bilevel optimization. Consider u to be the vector of non-negative importance values for each training example $u = [u_1, \dots, u_N]^T$ where N is the number of training examples, and w be the parameter(s) of a classifier $h(x; w)$. Then the weighted training error is $L_{w_train}(u, w) := \frac{1}{\sum_i u_i} \sum_{(x_i, y_i) \in \mathcal{D}_{train}} u_i l(h(x_i; w), y_i)$. Also, assume that we can get a small number of examples, from the same distribution as that of the test examples (clean validation examples). Then the importance learning problem can be formulated as:

$$\min_u L_{val}(u, w) \text{ s.t. } w = \arg \min_w L_{w_train}(u, w). \quad (3)$$

Hence, the importance of each training example (vector u) is selected such that the minimizer w of the weighted training loss in the lower level also minimizes the validation loss in the upper-level. The final importance values can help to identify good points from the noisy training set and the classifier w obtained after solving this optimization will have superior performance compared to the model trained on the noisy data.

Meta-learning. A standard learning problem involves finding the best model from the class of hypotheses for a given task (i.e., data distribution). In contrast, meta-learning is a problem of learning a prior on the hypothesis classes (a.k.a. inductive bias) for a given set of tasks. Few-shot learning is an example of meta-learning, where a learner is trained on several related tasks, during the meta-training phase, so that it can generalize well to unseen (but related) tasks with just few examples, during the meta-testing phase. An effective approach to the few-shot learning problem is to learn a common representation for various tasks and train task specific classifiers on top of this representation. Let T be the map that takes raw features to a common representation $T: \mathcal{X} \rightarrow \mathbb{R}^d$ for all tasks and h_i be the classifier for the i -th task, $i \in \{1, \dots, M\}$ where M is the total number of tasks for training. The goal of few-shot learning is to learn both the representation map $T(\cdot; u)$ parameterized by u and the set of classifiers $\{h_1, \dots, h_M\}$ parameterized by $w = \{w_1, \dots, w_M\}$. Let $L_{val}(u, w_i) := \frac{1}{N_{val}} \sum_{(x_i, y_i) \in \mathcal{D}_{val}} l(h_i(T(x_i; u); w_i), y_i)$ be the validation loss of task i and $L_{train}(u, w_i)$ be the training loss defined similarly, then the bilevel problem for few-shot learning is

$$\begin{aligned} & \min_u \sum_i L_{val}(u, w_i) \\ & \text{s.t. } w_i = \arg \min_{w_i} L_{train}(u, w_i), \quad i = 1, \dots, M. \end{aligned} \quad (4)$$

For evaluation of the learned representation, during the meta-test phase, the representation $T(\cdot; u)$ is kept fixed and only the classifiers for the new tasks $\{h'_1, \dots, h'_N\}$ are trained

i.e. $\min_{w'_i} L_{test}(u, w'_i)$ $i = 1, \dots, N$ where N is the total number of tasks for testing.

Training-data poisoning. Recently, machine learning models were shown to be vulnerable to train-time attacks. Different from the test time attacks, here adversary modifies the training data so that the model learned from altered training data performs poorly/differently as compared to the model learned from clean data. The most popular train-time attack method augments the original training data $X = \{x_1, \dots, x_N\}$ with one or more ‘poisoned’ examples $u = \{u_1, \dots, u_M\}$, i.e., $X' = X \cup u$ to create the poisoned dataset with $L_{poison}(u, w) := \frac{1}{N} \sum_{(x_i, y_i) \in X' \times Y} l(h(x_i; u, w), y_i)$ being the loss on the poisoned training data. The problem of finding poisoning points, that when added to the clean training data hurt the performance of the model trained on it can be formulated as

$$\min_u -L_{val}(u, w) \text{ s.t. } w = \arg \min_w L_{poison}(u, w), \quad (5)$$

where the minus sign in the upper-level is used to maximize the validation loss. This is the formulation for untargeted attacks. For targeted attacks, the upper-level must minimize the validation loss with respect to the intended target labels of the attacker. Another variant of poisoning attack, only influences the prediction of a single predetermined example. The upper-level cost for this attack is the loss over only this single example (see Eq. (10) in the Appendix D.4.1).

Challenges of deep bilevel optimization. General bilevel problems cannot be solved using simultaneous optimization of the upper- and lower-level problems. Moreover, exact bilevel optimization is known to be NP-hard even for linear cost functions [2]. To add to this, recent deep learning models, with millions of variables, make it infeasible to use sophisticated methods beyond the first-order methods. For bilevel problems, even the first-order methods are difficult to apply since they require computation of the inverse Hessian–gradient product to get the exact hypergradient (see Sec. 2.1). Since direct inversion of the Hessian is impractical, even for moderate-sized problems, many approaches have been proposed to approximate the exact hypergradient, including forward/reverse-mode differentiation [19; 10; 29], approximate inversion by solving a linear system of equations [8; 25]. But, there is still big room for improvement in these existing approaches in terms of their time and space complexities and practical performance.

Contributions. We propose a penalty function-based algorithm (Alg. 1) for solving large-scale unconstrained bilevel optimization. We prove its convergence under mild conditions (Theorem 2) and show that it computes the exact hypergradient asymptotically (Lemma 3). We present complexity analysis of the algorithm showing that it has linear time and constant space complexity (Table 1), making our

method superior to forward-mode and reverse-mode differentiation and similar to the approximate inversion based method. Small space and time complexity enables us to solve large-scale bilevel problems involving deep neural networks with up to 3.8M upper-level and 1.4M lower-level variables (Table 7 in Appendix). We show evaluation results on data denoising by importance learning, few-shot learning, and training-data poisoning problems. The proposed penalty-based method performs competitively to the state-of-the-art methods on simpler problems (with convex lower-level cost) and significantly outperforms other methods on complex problems (with non-convex lower-level cost), both in terms of accuracy (Sec. 3) and run-time (Table 2, Fig. 3).

The remainder of the paper is organized as follows. We present and analyze the main algorithm in Sec. 2, perform comprehensive experiments in Sec. 3, and conclude the paper in Sec. 4. Due to space limitation, proofs, experimental settings and additional results are presented in the appendix. All codes are published on GitHub <https://github.com/jihunham/bilevel-penalty>.

2. Inversion-Free Penalty Method

Throughout the paper we have assumed that upper- and lower-level costs f and g are twice continuously differentiable in both u and v . We use $\nabla_u f$ and $\nabla_v f$ to denote gradient vectors, $\nabla_{uv}^2 f$ for the matrix $\left[\frac{\partial^2 f}{\partial u_i \partial v_j}\right]$, and $\nabla_{vv}^2 f$ for the Hessian matrix $\left[\frac{\partial^2 f}{\partial v_i \partial v_j}\right]$. Additionally, following previous works we assumed that the lower-level solution $v^*(u) := \arg \min_v g(u, v)$ is unique for all u and that $\nabla_{vv}^2 g$ is invertible everywhere. Later in this section we discuss relaxation for some of these assumptions.

2.1. Hypergradient for bilevel optimization

Assuming we can express the solution to the lower-level problem $v^*(u) := \arg \min_v g(u, v)$ explicitly, we can write the bilevel problem as an equivalent single-level problem $\min_u f(u, v^*(u))$. We can use gradient-based approach on this single-level problem and compute the total derivative $\frac{df}{du}(u, v^*(u))$, called the hypergradient, in previous approaches. Using the chain rule, the total derivative is

$$\begin{aligned} \frac{df}{du}(u, v^*(u)) &= \nabla_u f(u, v^*(u)) \\ &+ \frac{dv}{du}(u, v^*(u)) \cdot \nabla_v f(u, v^*(u)) \end{aligned} \quad (6)$$

In reality, $v^*(u)$ can be written explicitly only for trivial problems, but we can still compute $\frac{dv}{du}$ using the implicit function theorem. Since $\nabla_v g = 0$ at $v = v^*(u)$, we get $du \cdot \nabla_{uv}^2 g + dv \cdot \nabla_{vv}^2 g = 0$ and consequently $\frac{dv}{du} = -\nabla_{uv}^2 g (\nabla_{vv}^2 g)^{-1}$. Thus, the hypergradient

is as follows

$$\frac{df}{du} = \nabla_u f + \frac{dv}{du} \nabla_v f = \nabla_u f - \nabla_{uv}^2 g (\nabla_{vv}^2 g)^{-1} \nabla_v f \quad (7)$$

Existing approaches [8; 19; 25; 10] can be viewed as implicit methods of approximating the hypergradient, with distinct trade-offs in efficiency and complexity.

2.2. Penalty function approach

A bilevel problem can be considered as a constrained optimization problem since the lower-level optimality $v = \arg \min_v g(u, v)$ is a constraint, in addition to any other constraint in the upper- and the lower-level problems. In this work, we focus on unconstrained bilevel problems i.e. those without any additional constraints on the upper- and lower-level problems. For solving bilevel problems the lower-level problem is often replaced by its necessary optimality condition, resulting in the following problem:

$$\min_{u,v} f(u, v), \quad \text{s.t.} \quad \nabla_v g(u, v) = 0 \quad (8)$$

For general bilevel problems, Eq. (8) and Eq. (1) are not the same [6]. But, with lower-level cost g being convex in v for each u and the assumption that the lower-level solution is unique for each u , Eq. (8) is equivalent to Eq. (1).

We now describe the penalty function approach for solving bilevel optimization. The penalty function method is a well-known approach for solving constrained optimization problems (see [5] for a review) and has been previously applied for solving bilevel problems. However, it was analyzed under strict assumptions and only high-level descriptions of the algorithm were presented before [1; 13]. The penalty function $\tilde{f}(u, v; \gamma) := f(u, v) + \frac{\gamma}{2} \|\nabla_v g(u, v)\|^2$, optimizes the original cost f plus a quadratic penalty term (penalizes the violation of the necessary conditions for lower-level optimality). Let (\hat{u}_k, \hat{v}_k) be the minimum of the penalty function \tilde{f} for a given γ_k :

$$\begin{aligned} (\hat{u}_k, \hat{v}_k) &:= \arg \min_{u,v} \tilde{f}(u, v; \gamma_k) \\ &= \arg \min_{u,v} f(u, v) + \frac{\gamma_k}{2} \|\nabla_v g(u, v)\|^2 \end{aligned} \quad (9)$$

Then the following convergence result is known.

Theorem 1 (Theorem 8.3.1 of [3]). *Assume f and g are convex in v for any fixed u . Let $\{\gamma_k\}$ be any positive ($\gamma_k > 0$) and divergent ($\gamma_k \rightarrow \infty$) sequence. If $\{(\hat{u}_k, \hat{v}_k)\}$ is the corresponding sequence of optimal solutions of the penalty function Eq. (9), then the sequence $\{(\hat{u}_k, \hat{v}_k)\}$ has limit points any one of which is a solution of Eq. (1).*

Even though this is a strong result, its not very practical, since the minimum (\hat{u}_k, \hat{v}_k) needs to be computed exactly for each γ_k , $k = 1, 2, \dots$, and moreover f and g need to be

convex in v for any u . In our approach, we allow ϵ_k -optimal solutions of Eq. (9) and show convergence to a KKT point of Eq. (8) without requiring convexity.

Theorem 2. *Suppose $\{\epsilon_k\}$ is a positive ($\epsilon_k > 0$) and convergent ($\epsilon_k \rightarrow 0$) sequence, and $\{\gamma_k\}$ is a positive ($\gamma_k > 0$), non-decreasing ($\gamma_1 \leq \gamma_2 \leq \dots$), and divergent ($\gamma_k \rightarrow \infty$) sequence. Let $\{(u_k, v_k)\}$ be the sequence of approximate solutions to Eq. (9) with tolerance $(\nabla_u \tilde{f}(u_k, v_k))^2 + (\nabla_v \tilde{f}(u_k, v_k))^2 \leq \epsilon_k^2$ for all $k = 0, 1, \dots$. Then any limit point of $\{(u_k, v_k)\}$ satisfies the KKT conditions of the problem in Eq. (8).*

Alg. 1 describes our method in which we minimize the penalty function in Eq. (9), alternatively over v and u . It is essential to note that our method solves a single-level penalty function (Eq. (9)) and does not need any intermediate step to compute the approximate hypergradient, unlike other methods which first approximate the solution to the lower-level problem of Eq. (1) and then use an intermediate step (solving a linear system or using reverse/forward mode differentiation) to compute the approximate hypergradient. Lemma 3 (below) shows when the approximate gradient direction $\nabla_u \tilde{f}$, computed from Alg. 1 becomes the exact hypergradient Eq. (7) for bilevel problems.

Lemma 3. *Given u , let \hat{v} be $\hat{v} := \arg \min_v \tilde{f}(u, v; \gamma)$ from Eq. (9). Then, $\nabla_u \tilde{f}(u, \hat{v}; \gamma) = \frac{df}{du}(u, \hat{v})$.*

Thus if we find the minimizer \hat{v} of the penalty function for given u and γ , Alg. 1 computes the exact hypergradient Eq. (7) at (u, \hat{v}) . Furthermore, under the conditions of Theorem 1, $\hat{v}(u) \rightarrow v^*(u)$ as $\gamma \rightarrow \infty$ and we get the exact hypergradient asymptotically.

Comparison with other methods: Many methods have been proposed previously to solve bilevel optimization problems that appear in machine learning, including forward/reverse-mode differentiation (FMD/RMD) [19; 10; 29] and approximate hypergradient computation by solving a linear system (ApproxGrad) [8; 25]. For completeness, we have described these methods briefly in Appendix B. We have shown the trade-offs of these methods for computing the hypergradient in Table 1. One can see that as T increases FMD and RMD become impractical due to $O(UV^2T)$ time complexity and $O(U + VT)$ space complexity, respectively, whereas ApproxGrad and Penalty, have the same linear time complexity and constant space complexity, which is a big advantage over FMD and RMD. However, complexity analysis does not show the quality of hypergradient approximation of each method. In Sec. 3.1 we show empirically that the proposed penalty method has better convergence properties than all the other methods with synthetic examples and since ApproxGrad and Penalty have the same complexities we compare the two methods on real data and show that Penalty is twice as fast as ApproxGrad (Fig. 3).

Algorithm 1 Penalty method for bilevel optimization

 Input: $K, T, \{\sigma_k\}, \{\rho_{k,t}\}, \gamma_0, \epsilon_0, c_\gamma(=1.1), c_\epsilon(=0.9)$

 Output: (u_K, v_T)

 Initialize u_0, v_0 randomly

Begin

 for $k = 0, \dots, K-1$ do

 while $\|\nabla_u \tilde{f}\|^2 + \|\nabla_v \tilde{f}\|^2 > \epsilon_k^2$ do

 for $t = 0, \dots, T-1$ do

 v-update: $v_{t+1} \leftarrow v_t - \rho_{k,t} \nabla_v \tilde{f}$ (from Eq. (9))

end for

 u-update: $u_{k+1} \leftarrow u_k - \sigma_k \nabla_u \tilde{f}$ (from Eq. (9))

end while

Break if max iteration is reached

 $\gamma_{k+1} \leftarrow c_\gamma \gamma_k, \quad \epsilon_{k+1} \leftarrow c_\epsilon \epsilon_k$

 end for

Improvements. A caveat to these theoretical guarantees is that, some of the assumptions made for analysis may not be satisfied in practice. Here we discuss simple techniques to address these problems and improve Alg. 1 further. The first problem is related to non-convexity of the lower-level cost g , which creates the problem that the local minimum of $\|\nabla_v g\|$ can be either a minimum or a maximum of g . To address this we modify the v -update for Eq. (9) by adding a ‘regularization’ term $\lambda_k g$ to the cost so that v finds a minimum of g . Thus, the v -update becomes $\min_v [f + \frac{\gamma_k}{2} \|\nabla_v g\|^2 + \lambda_k g]$. This only affects the optimization in the beginning; as $\lambda_k \rightarrow \infty$ the final solution remains unaffected with or without regularization. The second problem is that the tolerance $\nabla_{(u,v)} \tilde{f}(u_k, v_k; \gamma_k) \leq \epsilon_k$ may not be satisfied in a limited time and the optimization may terminate before γ_k becomes large enough. A cure to this is the method of multipliers and augmented Lagrangian [4] which allows the penalty method to find a solution with a finite γ_k . Thus we add the term $\nabla_v g^T \nu$ to the penalty function (Eq. (9)) to get $\min_{u,v} [f + \frac{\gamma_k}{2} \|\nabla_v g\|^2 + \nabla_v g^T \nu]$ and use the method of multiplier to update ν as $\nu \leftarrow \nu + \gamma \nabla_v g$. In summary, we use the following update rules in the paper.

$$u_{k+1} \leftarrow u_k - \rho \nabla_u \left[f + \frac{\gamma_k}{2} \|\nabla_v g\|^2 + \nabla_v g^T \nu_k \right]$$

$$v_{k+1} \leftarrow v_k - \sigma \nabla_v \left[f + \frac{\gamma_k}{2} \|\nabla_v g\|^2 + \nabla_v g^T \nu_k + \lambda_k g \right]$$

$$\nu_{k+1} \leftarrow \nu_k + \gamma_k \nabla_v g.$$

These improvements are helpful in theory but the empirical difference was only moderate (see Appendix C for details).

3. Experiments

In this section, we evaluate the performance of the proposed penalty method (Penalty) on various machine learning problems discussed in the introduction. We compare Penalty against both bilevel and non-bilevel solutions to these prob-

Table 1. Complexity analysis of various bilevel methods (FMD, RMD and ApproxGrad are discussed in Appendix B). U is the size of u , V is the size of v , and T is the total number of v -updates per one hypergradient computation. P , p , and q are variables of size $U \times V$, $U \times 1$, and $V \times 1$ required to compute the hypergradient (also updated T -times). Note: Hessian-gradient product has complexity $O(V)$ as shown in [24].

Method	v -update	Intermediate update	Time	Space
FMD	$v \leftarrow v - \rho \nabla_v g$	$P \leftarrow P(I - \rho \nabla_{vv}^2 g) - \rho \nabla_{uv}^2 g$	$O(UV^2T)$	$O(UV)$
RMD	$v \leftarrow v - \rho \nabla_v g$	$p \leftarrow p - \rho \nabla_{uv}^2 g \cdot q$ $q \leftarrow q - \rho \nabla_{vv}^2 g \cdot q$	$O(VT)$	$O(U + VT)$
ApproxGrad	$v \leftarrow v - \rho \nabla_v g$	$q \leftarrow q - \rho \nabla_{vv}^2 g [\nabla_{vv}^2 g \cdot q - \nabla_v f]$	$O(VT)$	$O(U+V)$
Penalty	$v \leftarrow v - \rho [\nabla_v f + \gamma \nabla_{vv}^2 g \nabla_v g]$	Not required	$O(VT)$	$O(U+V)$

lems previously reported in the literature.

3.1. Synthetic examples

We start by comparing Penalty (ours) with gradient descent (GD), reverse-mode differentiation (RMD), and approximate hypergradient method (ApproxGrad) on synthetic examples. We omit the comparison with forward-mode differentiation (FMD) because of its impractical time complexity for larger problems. GD refers to the alternating minimization: $u \leftarrow u - \rho \nabla_u f$, $v \leftarrow v - \sigma \nabla_v g$. For RMD, we implemented a simple version of the method using vanilla gradient descent. For ApproxGrad, we implement our own GPU compatible version (which uses Hessian-vector product, mini-batches and gradient descent rather than conjugate gradient descent for solving the linear system) of the algorithm proposed by [25]. Using simple quadratic surfaces for f and g , we compare all the algorithms by observing their convergence as a function of the number of upper-level iterations by varying the number of lower-level updates (T), for computing the hypergradient update. We measure the convergence of these methods using the Euclidean distance of the current iterate (u, v) from the closest optimal solution (u^*, v^*) . Since the synthetic examples are not learning problems, we can only measure the distance of the iterates to an optimal solution ($\|(u, v) - (u^*, v^*)\|_2^2$). Fig. 1 shows the performance of two 10-dimensional examples described in the caption (see Appendix D.1). As one would expect, increasing the number T of v -updates makes all the algorithms better since doing more lower-level iterations makes the hypergradient estimation more accurate (Eq. (7)) but it also increases the run time of the methods. However, even for these examples, only Penalty and ApproxGrad converge to the optimal solution and GD and RMD converge to non-solution points (regardless of T). Moreover, from Fig. 1(b), we see that Penalty converges even with $T=1$ while ApproxGrad requires at least $T=10$ to converge, which shows that our method approximates the hypergradient accurately with smaller T . This directly translates to smaller run-time for our method as compared to ApproxGrad since the run-time

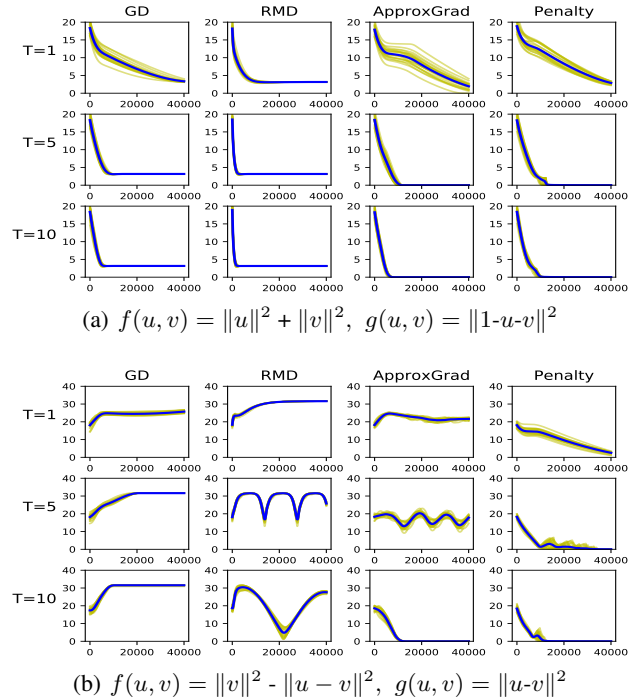


Figure 1. Convergence of GD, RMD, ApproxGrad, and Penalty for two example bilevel problems. The mean curve (blue) is superimposed on 20 independent trials (yellow).

is directly proportional to T (see Table. 1). In Fig. 2 we show examples similar to Fig. 1 but with ill-conditioned or singular Hessian $\nabla_{vv}^2 g$ for the lower-level problem. The ill-conditioning poses difficulty for the methods since the implicit function theorem requires the invertibility of the Hessian at the solution point. Compared to Fig. 1, Fig. 2 shows that only Penalty converges to the true solution despite the fact that we add regularization $\nabla_{vv}^2 g + \lambda I$ in ApproxGrad to improve the ill-conditioning when solving the linear systems by minimization. We ascribe the robustness of Penalty to its simplicity and to the fact that it naturally handles non-uniqueness of the lower-level solution (see Ap-

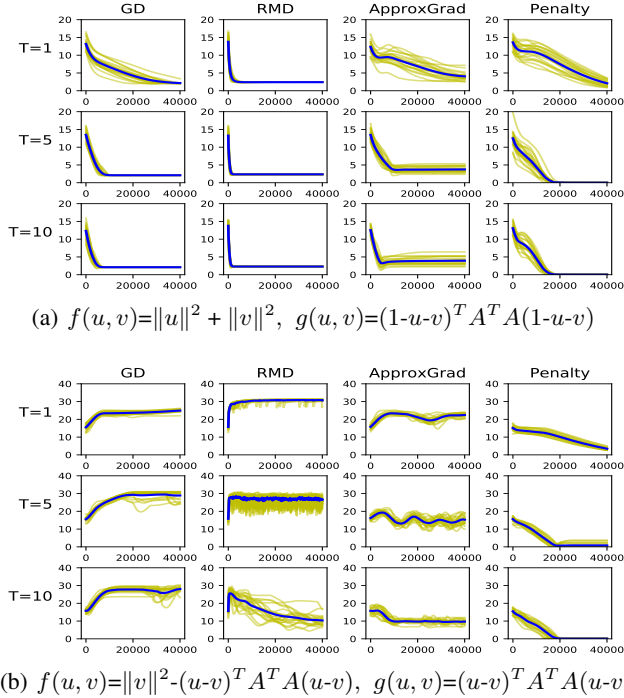


Figure 2. Convergence of GD, RMD, ApproxGrad, and Penalty for two example bilevel problems where $A^T A$ is a rank-deficient random matrix. The mean curve (blue) is superimposed on 20 independent trials (yellow).

pendix C.3). Additionally, we report the wall clock times for different methods on the four examples tested here in Table 2. We can see that as we increase the number of lower-level iterations all methods get slower but Penalty is faster than both RMD and ApproxGrad. Penalty is slower than GD but as shown in Fig. 1 and Fig. 2, GD does not converge to optima for most of the synthetic examples.

3.2. Data denoising by importance learning

Now, we evaluate the performance of Penalty for learning a classifier from a dataset with corrupted labels (training data). We pose the problem as an importance learning problem presented in Eq. (3). We evaluate the performance of the classifier learned by Penalty, with 20 lower-level updates, against the following classifiers: **Oracle**: classifier trained on the portion of training data with clean labels and the validation data, **Val-only**: classifier trained only on the validation data, **Train+Val**: classifier trained on the entire training and validation data, **ApproxGrad**: classifier trained with our implementation of ApproxGrad, with 20 lower-level and 20 linear system updates. We test the performance on MNIST, CIFAR10 and SVHN datasets with validation set sizes of 1000, 10000 and 1000 points respectively. We used convolutional neural networks (architectures described in

Table 2. Mean wall-clock time (sec) for 10,000 upper-level iterations for synthetic experiments. Boldface is the smallest among RMD, ApproxGrad, and Penalty. (Mean \pm s.d. of 10 runs)

Example 1	GD	RMD	ApproxGrad	Penalty
T=1	7.4 \pm 0.3	15.0\pm0.1	17.4 \pm 0.2	17.2 \pm 0.1
T=5	14.3 \pm 0.1	51.4 \pm 0.3	39.3 \pm 2.3	34.3\pm0.3
T=10	23.2 \pm 0.1	95.4 \pm 0.2	60.9 \pm 0.3	57.0\pm1.0
Example 2	GD	RMD	ApproxGrad	Penalty
T=1	7.7 \pm 0.1	18.5 \pm 0.1	17.2\pm0.3	17.4 \pm 0.2
T=5	17.3 \pm 0.1	62.7 \pm 0.1	37.9 \pm 0.1	35.0\pm0.2
T=10	22.4 \pm 2.6	115.0 \pm 0.4	64.2 \pm 0.3	52.7\pm1.4
Example 3	GD	RMD	ApproxGrad	Penalty
T=1	8.2 \pm 0.2	18.8\pm0.1	19.8 \pm 0.1	19.1 \pm 0.1
T=5	17.4 \pm 0.1	72.4 \pm 0.1	47.1 \pm 0.4	38.6\pm0.4
T=10	28.7 \pm 0.6	125.0 \pm 9.3	80.6 \pm 0.3	62.7\pm0.1
Example 4	GD	RMD	ApproxGrad	Penalty
T=1	7.9 \pm 0.1	19.5\pm0.1	20.4 \pm 0.0	19.6 \pm 0.1
T=5	16.9 \pm 0.2	72.8 \pm 0.5	48.4 \pm 0.6	40.2\pm0.1
T=10	28.3 \pm 0.2	138.0 \pm 0.2	81.2 \pm 1.6	58.0\pm4.3

Appendix D.2) at the lower-level for this task. Table 3 summarizes our results for this problem and shows that Penalty outperforms Val-only, Train+Val and ApproxGrad by significant margins and in fact performs very close to the Oracle classifier (which is the ideal classifier), even for high noise levels. This demonstrates that Penalty is extremely effective in solving bilevel problems involving several million variables (see Table 7 in Appendix) and shows its effectiveness at handling non-convex problems. Along with improvement in terms of accuracy over other bilevel methods like ApproxGrad, Penalty also gives better run-time per upper-level iteration, leading to a decrease in the overall run time of the experiments (Fig. 3(a)).

We compared the performance of Penalty against the RMD-based method presented in [10], using their setting from Sec. 5.1, which is a smaller version of this data denoising task. For this, we choose a sample of 5000 training, 5000 validation and 10000 test points from MNIST and randomly corrupted labels of 50% of the training points and used softmax regression in the lower-level of the bilevel formulation (Eq. (3)). The accuracy of the classifier trained on a subset of the dataset comprising only of points with importance values greater than 0.9 (as computed by Penalty) along with the validation set is 90.77%. This is better than the accuracy obtained by Val-only (90.54%), Train+Val (86.25%) and the RMD-based method (90.09%) used by [10] and is close to the accuracy achieved by Oracle classifier (91.06%).

3.3. Few-shot learning

Next, we evaluate the performance of Penalty on the task of learning a common representation for the few-shot learning

Table 3. Test accuracy (%) of the classifier learnt from datasets with noisy labels using importance learning. (Mean \pm s.d. of 5 runs)

Dataset (Noise%)	Oracle	Val-Only	Train+Val	Bilevel Approaches	
				ApproxGrad	Penalty
MNIST (25)	99.3 \pm 0.1	90.5 \pm 0.3	83.9 \pm 1.3	98.11 \pm 0.08	98.89 \pm 0.04
MNIST (50)	99.3 \pm 0.1	90.5 \pm 0.3	60.8 \pm 2.5	97.27 \pm 0.15	97.51 \pm 0.07
CIFAR10 (25)	82.9 \pm 1.1	70.3 \pm 1.8	79.1 \pm 0.8	71.59 \pm 0.87	79.67 \pm 1.01
CIFAR10 (50)	80.7 \pm 1.2	70.3 \pm 1.8	72.2 \pm 1.8	68.08 \pm 0.83	79.03 \pm 1.19
SVHN (25)	91.1 \pm 0.5	70.6 \pm 1.5	71.6 \pm 1.4	80.05 \pm 1.37	88.12 \pm 0.16
SVHN (50)	89.8 \pm 0.6	70.6 \pm 1.5	47.9 \pm 1.3	74.18 \pm 1.05	85.21 \pm 0.34

 Table 4. Few-shot classification accuracy (%) with Omniglot and Mini-ImageNet. We report mean \pm s.d. for Omniglot and 95% confidence intervals for Mini-Imagenet over five trials. For bilevel approaches (Penalty, ApproxGrad and RMD[11]) result is averaged over 600 randomly-sampled tasks from the meta-test set.

	Non-bilevel Approaches			Bilevel Approaches		
	MAML[9]	[31]	SNAIL[21]	RMD[11]	ApproxGrad	Penalty
Omniglot						
5-way 1-shot	98.7	98.8	99.1	98.6	97.49 \pm 0.31	97.57 \pm 0.11
5-way 5-shot	99.9	99.7	99.8	99.5	99.43 \pm 0.02	99.41 \pm 0.05
20-way 1-shot	95.8	96.0	97.6	95.5	93.07 \pm 0.24	92.20 \pm 0.22
20-way 5-shot	98.9	98.9	99.4	98.4	98.14 \pm 0.13	98.10 \pm 0.06
Mini-Imagenet						
5-way 1-shot	48.70 \pm 1.75	49.42 \pm 0.78	55.71 \pm 0.99	50.54 \pm 0.85	48.1 \pm 0.82	52.10 \pm 0.65
5-way 5-shot	63.11 \pm 0.92	68.20 \pm 0.66	68.88 \pm 0.92	64.53 \pm 0.68	64.9 \pm 0.84	66.91 \pm 0.92

problem. We use the formulation presented in Eq. (4) and use Omniglot [15] and Mini-ImageNet [32] datasets for our experiments. Following the protocol proposed by [32] for N -way K -shot classification, we generate meta-training and meta-testing datasets. Each meta-set is built using images from disjoint classes. For Omniglot, our meta-training set comprises of images from the first 1200 classes and the remaining 423 classes are used in the meta-testing dataset. We also augment the meta-datasets with three different rotations (90, 180 and 270 degrees) of the images as used by [28]. For the experiments with Mini-Imagenet, we used the split of 64 classes in meta-training, 16 classes in meta-validation and 20 classes in meta-testing as used by [26].

Each meta-batch of the meta-training and meta-testing dataset comprises of a number of tasks which is called the meta-batch-size. Each task in the meta-batch consists of a training set with K images and a testing set consists of 15 images from N classes. We train Penalty using a meta-batch-size of 30 for 5 way and 15 for 20 way classification for Omniglot and with a meta-batch-size of 2 for Mini-ImageNet experiments. The training sets of the meta-train-batch are used to train the lower-level problem and the test sets are used as validation sets for the upper-level problem in Eq. (4). The final accuracy is reported using the meta-test-set, for which we fix the common representation learnt during meta-training. We then train the classifiers at the lower-level for 100 steps using the training sets from the meta-test-batch and evaluate the performance of each task

on the associated test set from the meta-test-batch. Average performance of Penalty and ApproxGrad over 600 tasks is reported in Table 4. It can be seen that Penalty outperforms other bilevel methods namely the ApproxGrad (trained with 20 lower-level iterations and 20 updates for the linear system) and the RMD-based method [11] on Mini-Imagenet and is comparable to them on the Omniglot. We also show the trade-off between using higher T and time for ApproxGrad and Penalty in Fig. 3(b) showing that Penalty achieves the same accuracy as ApproxGrad in almost half the runtime. In comparison to non-bilevel approaches Penalty is comparable to most approaches but is slightly worse than [21] which makes use of temporal convolutions and soft attention.

We used four-layer convolutional neural networks with 64 filters per layer and a residual network with four residual blocks followed by two convolutional layers for learning the common task representation (upper-level variable) for Omniglot and Mini-ImageNet experiments, respectively. The lower-level problem uses logistic regression to learn the task specific classifiers (lower-level variables). We also use a normalization for the input-weight dot product, before taking the softmax, similar to the cosine normalization proposed by [18]. The bilevel problem for Mini-ImageNet has 3.8M upper-level variables which is the largest among all the experiments presented in this paper (Table 7 in Appendix).

Table 5. Test accuracy (%) of untargeted poisoning attack (LEFT) and success rate (%) of targeted attack (RIGHT), using MNIST and logistic regression. (Mean \pm s.d. of 5 runs)

Untargeted Attacks (lower accuracy is better)				
Poisoned points	Label flipping	RMD [22]	ApproxGrad	Penalty
1%	86.71 \pm 0.32	85	82.09 \pm 0.84	83.29 \pm 0.43
2%	86.23 \pm 0.98	83	77.54 \pm 0.57	78.14 \pm 0.53
3%	85.17 \pm 0.96	82	74.41 \pm 1.14	75.14 \pm 1.09
4%	84.93 \pm 0.55	81	71.88 \pm 0.40	72.70 \pm 0.46
5%	84.39 \pm 1.06	80	68.69 \pm 0.86	69.48 \pm 1.93
6%	84.64 \pm 0.69	79	66.91 \pm 0.89	67.59 \pm 1.17
Targeted Attacks (higher accuracy is better)				
Poisoned points	Label flipping	RMD [22]	ApproxGrad	Penalty
1%	7.76 \pm 1.07	10	18.84 \pm 1.90	17.40 \pm 3.00
2%	12.08 \pm 2.13	15	39.64 \pm 3.72	41.64 \pm 4.43
3%	18.36 \pm 1.23	25	52.76 \pm 2.69	51.40 \pm 2.72
4%	24.41 \pm 2.05	35	60.01 \pm 1.61	61.16 \pm 1.34
5%	30.41 \pm 4.24	-	65.61 \pm 4.01	65.52 \pm 2.85
6%	32.88 \pm 3.47	-	71.48 \pm 4.24	70.01 \pm 2.95

3.4. Training-data poisoning

Next, we evaluate Penalty on the task of generating poisoned training data, such that models trained on this data, perform poorly/differently as compared to the models trained on the clean data [20; 22; 14]. We use the same setting as Sec. 4.2 of [22] and test both untargeted and targeted data poisoning on MNIST using data augmentation technique. Here, we assume regularized logistic regression will be used as the classifier during training. The poisoned points obtained after solving Eq. (5) by various methods are added to the clean training set and the performance of a new classifier trained on this data is used to report the results in Table 5. For untargeted attack, our aim is to generally lower the performance of the classifier on the clean test set. For this experiment, we select a random subset of 1000 training, 1000 validation and 8000 testing points from MNIST and initialize the poisoning points with random instances from the training set but assign them incorrect random labels. We use these poisoned points along with clean training data to train logistic regression, in the lower-level problem of Eq. (5). For targeted attacks, we aim to misclassify images of eights as threes. For this, we selected a balanced subset (each of the 10 classes are represented equally in the subset) of 1000 training, 4000 validation and 5000 testing points from the MNIST dataset. Then we select images of class 8 from the validation set and label them as 3 and use only these images for the upper-level problem in Eq. 5 with a difference that now we want to minimize the error in the upper level instead of maximizing (meaning we don't have a negative sign in the upper level of Eq. 5). To evaluate the performance we selected images of 8 from the test set

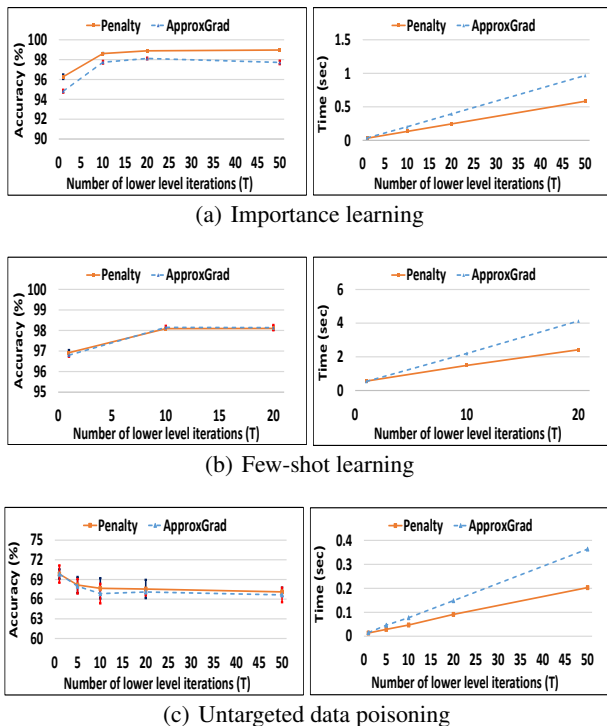


Figure 3. Comparison of accuracy and wall clock time (per upper-level iteration) with number of lower-level iterations T of Penalty and ApproxGrad (For ApproxGrad, we perform T updates for the linear system) on data denoising problem (Sec. 3.2 with 25% noise on MNIST), few-shot learning problem (Sec. 3.3 with 20 way 5 shot classification on Omniglot) and untargeted data poisoning (Sec. 3.4 with 60 poisoned points on MNIST).

and labeled them as 3 and report the performance on this modified subset of the original test set in targeted attack section of Table 5. For this experiment the poisoned points are initialized with images of classes 3 and 8 from the training set, with flipped labels. We did this since images of threes and eights are the only ones involved in the poisoning. We compare the performance of Penalty against the performance reported using RMD in [22] and ApproxGrad. For ApproxGrad, we used 20 lower-level and 20 linear system updates to report the results in the Table 5. We see that Penalty significantly outperforms the RMD based method and performs similar to ApproxGrad. However, in terms of wall clock time Penalty has a advantage over ApproxGrad (see Fig. 3(c)). We also compared the methods against a label flipping baseline where we select poisoned points from the validation sets and change their labels (randomly for untargeted attacks and mislabel threes as 8 and eights as 3 for targeted attacks). All bilevel methods are able to beat this baseline showing that solving the bilevel problem can generate much better poisoning points. Examples of the poisoned points for untargeted and targeted attacks generated by Penalty are shown in Figs. 5 and 6 in Appendix D.4.

Additionally, we tested Penalty on the task of generating clean label poisoning attack [14; 30] where goal is to learn poisoned points, such that they will be assigned correct labels when visually inspected by an expert, but can cause misclassification of specific target images when the classifier is trained on these poisoned points along with clean data. We used the dog vs. fish dataset and followed the setting in Sec. 5.2 of [14], to achieve 100% attack success with just a single poisoned point per target image, compared to 57% attack success in the original paper. A recent method [30] also reports 100% attack success on this same task. Details of the experiment are presented in Appendix D.4.1.

3.5. Impact of T on accuracy and wall-clock time

Finally, we compare Penalty and ApproxGrad on accuracy and time in Fig. 3 as we vary the number of lower-level iterations T in the experiments. Intuitively, a larger T corresponds to a more accurate approximation of the hyper-gradient and therefore a better result for all methods, but it comes with the space and time cost. The figure shows that relative improvement after $T = 20$ is small in comparison to the increased run-time for both Penalty and ApproxGrad. Based on this result we used $T = 20$ for in all our experiments on real data. The figure also shows that even though Penalty and ApproxGrad have the same linear time complexity (Table 1), Penalty is about twice as fast ApproxGrad in wall-clock time.

4. Conclusion

A wide range of interesting machine learning problems can be expressed as bilevel optimization problems, and new applications are still being discovered. So far, the difficulty of solving bilevel optimization has limited its wide-spread use for solving large-scale problems, specially, involving deep models. In this paper we presented an efficient algorithm based on penalty function to solve bilevel optimization, which is both simple and has theoretical and practical advantages over existing methods. As compared to previous methods we demonstrated competitive performance on problems with convex lower-level costs and significant improvement on problems with non-convex lower-level costs both in terms of accuracy and time, highlighting the practical effectiveness of our penalty-based method. In future works, we plan to tackle other challenges in bilevel optimization such as handling additional constraints in both upper- and lower-levels.

References

- [1] E. Aiyoshi and K. Shimizu. A solution method for the static constrained stackelberg problem via penalty method. *IEEE Transactions on Automatic Control*, 29(12):1111–1114, 1984.
- [2] J. F. Bard. Some properties of the bilevel programming problem. *Journal of optimization theory and applications*, 68(2):371–378, 1991.
- [3] J. F. Bard. *Practical bilevel optimization: algorithms and applications*, volume 30. Springer Science & Business Media, 2013.
- [4] D. P. Bertsekas. On penalty and multiplier methods for constrained minimization. *SIAM Journal on Control and Optimization*, 14(2):216–235, 1976.
- [5] D. P. Bertsekas. Nonlinear programming. *Journal of the Operational Research Society*, 48(3):334–334, 1997.
- [6] S. Dempe and J. Dutta. Is bilevel programming a special case of a mathematical program with complementarity constraints? *Mathematical programming*, 131(1-2):37–48, 2012.
- [7] J. Deng, W. Dong, R. Socher, L.-J. Li, K. Li, and L. Fei-Fei. Imagenet: A large-scale hierarchical image database. In *2009 IEEE conference on computer vision and pattern recognition*, pages 248–255. Ieee, 2009.
- [8] J. Domke. Generic methods for optimization-based modeling. In *Artificial Intelligence and Statistics*, pages 318–326, 2012.
- [9] C. Finn, P. Abbeel, and S. Levine. Model-agnostic meta-learning for fast adaptation of deep networks. In *International Conference on Machine Learning*, pages 1126–1135, 2017.
- [10] L. Franceschi, M. Donini, P. Frasconi, and M. Pontil. Forward and reverse gradient-based hyperparameter optimization. In *International Conference on Machine Learning*, pages 1165–1173, 2017.
- [11] L. Franceschi, P. Frasconi, S. Salzo, R. Grazzi, and M. Pontil. Bilevel programming for hyperparameter optimization and meta-learning. In *International Conference on Machine Learning*, pages 1563–1572, 2018.
- [12] J. Hamm and Y.-K. Noh. K-beam minimax: Efficient optimization for deep adversarial learning. *International Conference on Machine Learning (ICML)*, 2018.
- [13] Y. Ishizuka and E. Aiyoshi. Double penalty method for bilevel optimization problems. *Annals of Operations Research*, 34(1):73–88, 1992.

- [14] P. W. Koh and P. Liang. Understanding black-box predictions via influence functions. In *International Conference on Machine Learning*, pages 1885–1894, 2017.
- [15] B. M. Lake, R. Salakhutdinov, and J. B. Tenenbaum. Human-level concept learning through probabilistic program induction. *Science*, 350(6266):1332–1338, 2015.
- [16] T. Liu and D. Tao. Classification with noisy labels by importance reweighting. *IEEE Transactions on pattern analysis and machine intelligence*, 38(3):447–461, 2016.
- [17] J. Luketina, M. Berglund, K. Greff, and T. Raiko. Scalable gradient-based tuning of continuous regularization hyperparameters. In *International Conference on Machine Learning*, pages 2952–2960, 2016.
- [18] C. Luo, J. Zhan, X. Xue, L. Wang, R. Ren, and Q. Yang. Cosine normalization: Using cosine similarity instead of dot product in neural networks. In *International Conference on Artificial Neural Networks*, pages 382–391. Springer, 2018.
- [19] D. Maclaurin, D. Duvenaud, and R. Adams. Gradient-based hyperparameter optimization through reversible learning. In *International Conference on Machine Learning*, pages 2113–2122, 2015.
- [20] S. Mei and X. Zhu. Using machine teaching to identify optimal training-set attacks on machine learners. In *AAAI*, pages 2871–2877, 2015.
- [21] N. Mishra, M. Rohaninejad, X. Chen, and P. Abbeel. A simple neural attentive meta-learner. *arXiv preprint arXiv:1707.03141*, 2017.
- [22] L. Muñoz-González, B. Biggio, A. Demontis, A. Paudice, V. Wongrassamee, E. C. Lupu, and F. Roli. Towards poisoning of deep learning algorithms with back-gradient optimization. In *Proceedings of the 10th ACM Workshop on Artificial Intelligence and Security*, pages 27–38. ACM, 2017.
- [23] J. Nocedal and S. Wright. *Numerical optimization*. Springer Science & Business Media, 2006.
- [24] B. A. Pearlmutter. Fast exact multiplication by the hessian. *Neural computation*, 6(1):147–160, 1994.
- [25] F. Pedregosa. Hyperparameter optimization with approximate gradient. In *International conference on machine learning*, pages 737–746, 2016.
- [26] S. Ravi and H. Larochelle. Optimization as a model for few-shot learning. *International Conference on Learning Representations (ICLR)*, 2017.
- [27] M. Ren, W. Zeng, B. Yang, and R. Urtasun. Learning to reweight examples for robust deep learning. In *ICML*, 2018.
- [28] A. Santoro, S. Bartunov, M. Botvinick, D. Wierstra, and T. Lillicrap. One-shot learning with memory-augmented neural networks. *arXiv preprint arXiv:1605.06065*, 2016.
- [29] A. Shaban, C.-A. Cheng, N. Hatch, and B. Boots. Truncated back-propagation for bilevel optimization. *arXiv preprint arXiv:1810.10667*, 2018.
- [30] A. Shafahi, W. R. Huang, M. Najibi, O. Suciuc, C. Studer, T. Dumitras, and T. Goldstein. Poison frogs! targeted clean-label poisoning attacks on neural networks. In *Advances in Neural Information Processing Systems*, pages 6103–6113, 2018.
- [31] J. Snell, K. Swersky, and R. Zemel. Prototypical networks for few-shot learning. In *Advances in Neural Information Processing Systems*, pages 4080–4090, 2017.
- [32] O. Vinyals, C. Blundell, T. Lillicrap, D. Wierstra, et al. Matching networks for one shot learning. In *Advances in Neural Information Processing Systems*, pages 3630–3638, 2016.
- [33] H. Von Stackelberg. *Market structure and equilibrium*. Springer Science & Business Media, 2010.
- [34] X. Yu, T. Liu, M. Gong, K. Zhang, and D. Tao. Transfer learning with label noise. *arXiv preprint arXiv:1707.09724*, 2017.

Appendix

We provide missing proofs in Appendix A, a review of other methods of hypergradient computation in Appendix B, discuss modifications to improve the Alg. 1 in Appendix C, and the experiment details and additional results in Appendix D.

A. Proofs

Theorem 2. *Suppose $\{\epsilon_k\}$ is a positive ($\epsilon > 0$) and convergent ($\epsilon_k \rightarrow 0$) sequence, and $\{\gamma_k\}$ is a positive ($\gamma_k > 0$), non-decreasing ($\gamma_1 \leq \gamma_2 \leq \dots$), and a divergent ($\gamma_k \rightarrow \infty$) sequence. Let $\{(u_k, v_k)\}$ be the sequence of approximate solutions to Eq. (9) with tolerance $(\nabla_u \tilde{f}(u_k, v_k))^2 + (\nabla_v \tilde{f}(u_k, v_k))^2 \leq \epsilon_k^2$ for all $k = 0, 1, \dots$. Then any limit point of $\{(u_k, v_k)\}$ satisfies the KKT conditions of the problem Eq. (8).*

Proof. The proof follows the standard proof for penalty function methods, e.g., [23]. Let $w := (u, v)$ refer to the pair, and let $\bar{w} := (\bar{u}, \bar{v})$ be any limit point of the sequence $\{w_k := (u_k, v_k)\}$, then there is a subsequence \mathcal{K} such that $\lim_{k \in \mathcal{K}} w_k = \bar{w}$. From the tolerance condition

$$\begin{aligned} \|\nabla_w \tilde{f}(w_k; \gamma_k)\| &= \\ \|\nabla_w f(w_k) + \gamma_k \nabla_{wv}^2 g(w_k) \nabla_v g(w_k)\| &\leq \epsilon_k \end{aligned}$$

we have

$$\|\nabla_{wv}^2 g(w_k) \nabla_v g(w_k)\| \leq \frac{1}{\gamma_k} [\|\nabla_w f(w_k)\| + \epsilon_k]$$

Take the limit with respect to the subsequence \mathcal{K} on both sides to get

$$\nabla_{wv}^2 g(\bar{w}) \nabla_v g(\bar{w}) = 0$$

Since $\nabla_{wv}^2 g = \begin{pmatrix} \nabla_{uv}^2 g \\ \nabla_{vv}^2 g \end{pmatrix}$ is a tall matrix and $\nabla_{vv}^2 g$ is invertible by assumption, $\nabla_{wv}^2 g$ is full-rank and therefore $\nabla_v g(\bar{w}) = 0$, which is the primary feasibility condition in Eq. (8). Furthermore, let $\mu_k := -\gamma_k \nabla_v g(w_k)$, then by definition,

$$\nabla_w \tilde{f}(w_k; \gamma_k) = \nabla_w f(w_k) - \nabla_{wv}^2 g(w_k) \mu_k$$

We can write

$$\begin{aligned} &[\nabla_{wv}^2 g(w_k)^T \nabla_{wv}^2 g(w_k)] \mu_k = \\ &\nabla_{wv}^2 g(w_k)^T [\nabla_w f(w_k) - \nabla_w \tilde{f}(w_k; \gamma_k)] \end{aligned}$$

The corresponding limit $\bar{\mu}$ can be found by taking the limit of the subsequence \mathcal{K}

$$\begin{aligned} \bar{\mu} &:= \lim_{k \in \mathcal{K}} \mu_k = \\ &[\nabla_{wv}^2 g(\bar{w})^T \nabla_{wv}^2 g(\bar{w})]^{-1} \nabla_{wv}^2 g(\bar{w})^T \nabla_w f(\bar{w}) \end{aligned}$$

Since $\lim_{k \in \mathcal{K}} \nabla_w \tilde{f}(w_k; \gamma_k) = 0$ from the condition $\epsilon_k \rightarrow 0$, we get

$$\nabla_w f(\bar{w}) - \nabla_{wv}^2 g(\bar{w}) \bar{\mu} = 0$$

at the limit \bar{w} , which is the stationarity condition of Eq. (8). Together with the feasibility condition $\nabla_v g(\bar{w}) = 0$, the two KKT conditions of Eq. (8) are satisfied at the limit point. \square

Lemma 3. *Given u , let \hat{v} be $\hat{v} := \arg \min_v \tilde{f}(u, v; \gamma)$ of Eq. (9). Then, $\nabla_u \tilde{f}(u, \hat{v}; \gamma) = \frac{df}{du}(u, \hat{v})$.*

Proof. At the minimum \hat{v} the gradient $\nabla_v \tilde{f}$ vanishes, that is $\nabla_v f + \gamma \nabla_{vv}^2 g \nabla_v g = 0$. Equivalently, $\nabla_v g = -\gamma^{-1} (\nabla_{vv}^2 g)^{-1} \nabla_v f$. Then,

$$\begin{aligned} \nabla_u \tilde{f}(\hat{v}) &= \nabla_u f(\hat{v}) + \gamma \nabla_{uv}^2 g(\hat{v}) \nabla_v g(\hat{v}) = \\ \nabla_u f(\hat{v}) - \nabla_{uv}^2 g(\hat{v}) \nabla_{vv}^2 g^{-1}(\hat{v}) \nabla_v f(\hat{v}), \end{aligned}$$

where γ disappears, which is the hypergradient $\frac{df}{du}(u, \hat{v})$. \square

That is, if we find the minimum \hat{v} of the penalty function for given u and γ , we get the hypergradient Eq. (7) at (u, \hat{v}) . Furthermore, under the conditions of Theorem 1, $\hat{v}(u) \rightarrow v^*(u)$ as $\gamma \rightarrow \infty$ (see Lemma 8.3.1 of [3]), and we get the exact hypergradient asymptotically.

B. Review of bilevel optimization methods

Several methods have been proposed to solve bilevel optimization problems appearing in machine learning, including forward/reverse-mode differentiation [19; 10] and approximate gradient [8; 25] described briefly here.

Forward-mode (FMD) and Reverse-mode differentiation (RMD). Domke [8], Maclaurin et al. [19], Franceschi et al. [10], and Shaban et al. [29] studied forward and reverse-mode differentiation to solve the minimization problem $\min_u f(u, v)$ where the lower-level variable v follows a dynamical system $v_{t+1} = \Phi_{t+1}(v_t; u)$, $t = 0, 1, 2, \dots, T - 1$. This setting is more general than that of a bilevel problem. However, a stable dynamical system is one that converges to a steady state and thus, the process $\Phi_{t+1}(\cdot)$ can be considered as minimizing an energy or a potential function.

Define $A_{t+1} := \nabla_v \Phi_{t+1}(v_t)$ and $B_{t+1} := \nabla_u \Phi_{t+1}(v_t)$, then the hypergradient Eq. (7) can be computed by

$$\frac{df}{du} = \nabla_u f(u, v_T) + \sum_{t=0}^{T-1} B_t A_{t+1} \times \dots \times A_T \nabla_v f(u, v_T)$$

When the lower-level process is one step of gradient descent on a cost function g , that is,

$$\Phi_{t+1}(v_t; u) = v_t - \rho \nabla_v g(u, v_t)$$

we get

$$A_{t+1} = I - \rho \nabla_{vv}^2 g(u, v_t), \quad B_{t+1} = -\rho \nabla_{uv}^2 g(u, v_t).$$

The sequences $\{A_t\}$ and $\{B_t\}$ can be computed in forward or reverse mode. For reverse-mode differentiation, first compute

$$v_{t+1} = \Phi_{t+1}(v_t), \quad t = 0, 1, \dots, T-1,$$

then compute

$$\begin{aligned} q_T &\leftarrow \nabla_v f(u, v_T), \quad p_T \leftarrow \nabla_u f(u, v_T) \\ p_{t-1} &\leftarrow p_t + B_t q_t, \quad q_{t-1} \leftarrow A_t q_t, \quad t = T, T-1, \dots, 1. \end{aligned}$$

The final hypergradient is $\frac{df}{du} = p_0$. For forward-mode differentiation, simultaneously compute v_t, A_t, B_t and

$$Z_0 \leftarrow 0, \quad Z_{t+1} \leftarrow Z_t A_{t+1} + B_{t+1}, \quad t = 0, 1, \dots, T-1.$$

The final hypergradient is

$$\frac{df}{du} = \nabla_u f(u, v_T) + Z_T \nabla_v f(v_T).$$

Approximate hypergradient (ApproxGrad). Since computing the inverse of the Hessian $(\nabla_{vv}^2 g)^{-1}$ directly is difficult even for moderately-sized neural networks, Domke [8] proposed to find an approximate solution to $q = (\nabla_{vv}^2 g)^{-1} \nabla_v f$ by solving the linear system of equations $\nabla_{vv}^2 g \cdot q \approx \nabla_v f$. This can be done by solving

$$\min_q \|\nabla_{vv}^2 g \cdot q - \nabla_v f\|$$

using conjugate gradient or any other method. Note that the minimization requires evaluation of the Hessian-vector product, which can be done in linear time [24]. The asymptotic convergence with approximate solutions was shown by Pedregosa [25].

C. Improvements to Algorithm 1

Here we discuss the details of the modifications to Alg. 1 presented in the main text which can be added to improve the performance of the algorithm in practice.

C.1. Improving local convexity by regularization

One of the common assumptions of this and previous works is that $\nabla_{vv}^2 g$ is invertible and locally positive definite. Neither invertibility nor positive definiteness hold in general for bilevel problems, involving deep neural networks, and this causes difficulties in the optimization. Note that if g is non-convex in v , minimizing the penalty term $\|\nabla_v g\|$ does not necessarily lower the cost g but instead moves the variable towards a stationary point – which is a known problem even

for the Newton’s method. Thus we propose the following modification to the v -update:

$$\min_v \left[f + \frac{\gamma_k}{2} \|\nabla_v g\|^2 + \lambda_k g \right]$$

keeping the same u -update intact. To see how this affects the optimization, note that v -update becomes

$$v \leftarrow v - \rho \left[f_v + \gamma_k \nabla_{vv}^2 g \nabla_v g + \lambda_k \nabla_v g \right]$$

After v converges to a stationary point, we get $\nabla_v g = -(\gamma_k \nabla_{vv}^2 g + \lambda_k I)^{-1} \nabla_v f$, and after plugging this into u -update, we get

$$u \leftarrow u - \sigma \left[\nabla_u f - \nabla_{uv}^2 g \left(\nabla_{vv}^2 g + \frac{\lambda_k}{\gamma_k} I \right)^{-1} \nabla_v f \right]$$

that is, the Hessian inverse $\nabla_{vv}^2 g^{-1}$ is replaced by a regularized version $(\nabla_{vv}^2 g + \frac{\lambda_k}{\gamma_k} I)^{-1}$ to improve the positive definiteness of the Hessian. With a decreasing or constant sequence $\{\lambda_k\}$ such that $\lambda_k/\gamma_k \rightarrow 0$ the regularization does not change to solution.

C.2. Convergence with finite γ_k

The penalty function method is intuitive and easy to implement, but the sequence $\{(\hat{u}_k, \hat{v}_k)\}$ is guaranteed to converge to an optimal solution only in the limit with $\gamma \rightarrow \infty$, which may not be achieved in practice in a limited time. It is known that the penalty method can be improved by introducing an additional term into the function, which is called the augmented Lagrangian (penalty) method [4]:

$$\min_{u,v} \left[f + \frac{\gamma_k}{2} \|\nabla_v g\|^2 + \nabla_v g^T \nu \right].$$

This new term $\nabla_v g^T \nu$ allows convergence to the optimal solution (u^*, v^*) even when γ_k is finite. Furthermore, using the update rule $\nu \leftarrow \nu + \gamma \nabla_v g$, called the method of multipliers, it is known that ν converges to the true Lagrange multiplier of this problem corresponding to the equality constraints $\nabla_v g = 0$.

C.3. Non-unique lower-level solution

Most existing methods have assumed that the lower-level solution $\arg \min_v g(u, v)$ is unique for all u . Regularization from the previous section, can improve the ill-conditioning of the Hessian $\nabla_{vv}^2 g$ but it does not address the case of multiple disconnected global minima of g . With multiple lower-level solutions $V(u) = \{v \mid v = \arg \min g(u, v)\}$, there is an ambiguity in defining the upper-level problem. If we assume that $v \in V(u)$ is chosen adversarially (or pessimistically), then the upper-level problem should be defined as

$$\min_u \max_{v \in V(u)} f(u, v).$$

If $v \in V(u)$ is chosen co-operatively (or optimistically), then the upper-level problem should be defined as

$$\min_u \min_{v \in V(u)} f(u, v),$$

and the results can be quite different between these two cases. Note that the proposed penalty function method is naturally solving the optimistic case, as Alg. 1 is solving the problem of $\min_{u,v} \tilde{f}(u, v)$ by alternating gradient descent. However, with a gradient-based method, we cannot hope to find all disconnected multiple solutions. In a related problem of min-max optimization, which is a special case of bilevel optimization, an algorithm for handling non-unique solutions was proposed recently [12]. This idea of keeping multiple candidate solution may be applicable to bilevel problems too and further analysis of the non-unique lower-level problem is left as future work.

C.4. Modified algorithm

Here we present the modified algorithm which incorporates regularization (Sec. C.1) and augmented Lagrangian (Sec. C.2) as discussed previously. The augmented Lagrangian term $\nabla_v g^T \nu$ applies to both u - and v -update, but the regularization term λg applies to only the v -update as its purpose is to improve the ill-conditioning of $\nabla_{vv}^2 g$ during v -update. The modified penalized functions \tilde{f}_1 for u -update and \tilde{f}_2 for v -update are

$$\begin{aligned} \tilde{f}_1(u, v; \gamma, \nu) &:= f + \frac{\gamma}{2} \|\nabla_v g\|^2 + \nabla_v g^T \nu \\ \tilde{f}_2(u, v; \gamma, \lambda, \nu) &:= f + \frac{\gamma}{2} \|\nabla_v g\|^2 + \nabla_v g^T \nu + \lambda g \end{aligned}$$

The new algorithm (Alg. 2) is similar to Alg. 1 with additional steps for updating λ_k and ν_k .

C.5. Impact of various hyperparameters and terms

Here we evaluate the impact of different initial values for the hyperparameters and impact of different terms added in the modified algorithm (Algorithm 2). In particular, we examine the effect of using different initial values of λ_0 for synthetic experiments and λ_0, γ_0 for untargeted data poisoning with 60 points and also test the effect of having the $\lambda_k g$ and $\nabla_v g^T \nu$ (Fig. 4 and Table 6). Based on the results we see initial value of the regularization parameter λ_0 does not influence the results too much and absence of $\lambda_k g$ ($\lambda_k=0$) also does not change the results too much. We also don't see significant gains from using the augmented Lagrangian term and method of multipliers on these simple problems. However, the initial value of the parameter γ_0 does influence the results since starting from very large γ_0 makes the algorithm focus only on satisfying the necessary condition at the lower level ignoring the f where as with small γ_0 it can take a large number of iterations for the

Algorithm 2 Modified Alg. 1 with regularization and augmented Lagrangian

Input: $K, T, \{\sigma_k\}, \{\rho_{k,t}\}, \gamma_0, \epsilon_0, \lambda_0, \nu_0, c_\gamma (=1.1), c_\epsilon (=0.9), c_\lambda (=0.9)$

Output: (u_K, v_T)

Initialize u_0, v_0 randomly

Begin

```

for  $k = 0, \dots, K-1$  do
  while  $\|\nabla_u \tilde{f}_1\|^2 + \|\nabla_v \tilde{f}_2\|^2 > \epsilon_k^2$  do
    for  $t = 0, \dots, T-1$  do
       $v_{t+1} \leftarrow v_t - \rho_{k,t} \nabla_v \tilde{f}_2(u_k, v_t)$ 
    end for
     $u_{k+1} \leftarrow u_k - \sigma_k \nabla_u \tilde{f}_1(u_k, v_T)$ 
  end while
  Break if max iteration is reached
   $\gamma_{k+1} \leftarrow c_\gamma \gamma_k$ 
   $\epsilon_{k+1} \leftarrow c_\epsilon \epsilon_k$ 
   $\lambda_{k+1} \leftarrow c_\lambda \lambda_k$ 
   $\nu_{k+1} \leftarrow \nu_k + \gamma_k \nabla_v g$ 
end for
    
```

Table 6. Effect of using different initial values for various hyperparameters with Penalty on untargeted data poisoning attacks with 60 poisoning points (Mean \pm s.d. of 5 runs with $T = 20$ (lower-level iterations)). We used the parameters corresponding to the bold values for the results reported in Table 5.

Hyper-parameters	Different values of various Hyper-parameters			
	$\lambda_0 = 0$	$\lambda_0 = 1$	$\lambda_0 = 10$	$\lambda_0 = 100$
λ_0	67.87 \pm 1.35	68.21 \pm 1.78	68.18 \pm 1.04	67.59 \pm 1.17
ν	with ν		without ν	
	67.59 \pm 1.17		68.82 \pm 0.75	
γ_0	$\gamma_0 = 1$	$\gamma_0 = 10$		$\gamma_0 = 100$
	73.38 \pm 4.98	67.59 \pm 1.17		71.96 \pm 3.56

penalty term to have influence. Apart from these, we also tested the effects of the rate of tolerance decrease (c_ϵ) and penalty increase (c_γ), and initial value for ϵ_0 . Within certain ranges, the results do not change much.

D. Details of experiments

All codes are written in Python using Tensorflow/Keras, and were run on Intel CORE i9-7920X CPU with 128 GB of RAM and dual NVIDIA TITAN RTX. Implementation and hyperparameters of the algorithms are experiment-dependent and described separately below.

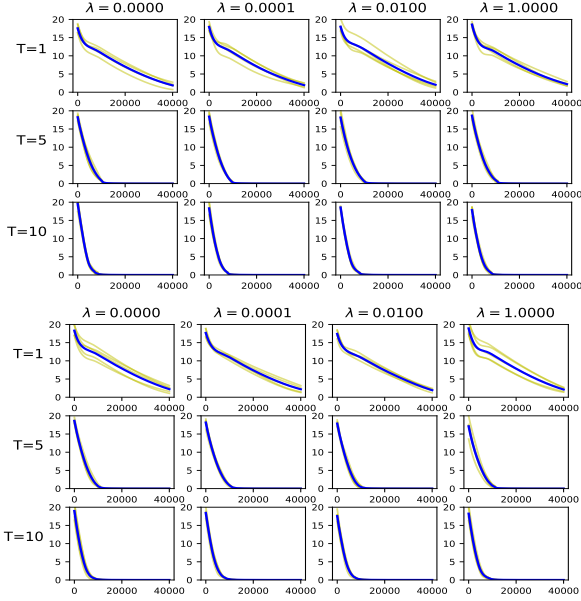


Figure 4. Penalty method for $T=1,5,10$ and $\lambda_0 = 0, 10^{-4}, 10^{-2}, 1$ for Example 1 of Sec.3.1. Left: with ν . Right: without ν . Averaged over 5 trials.

Table 7. Upper- and lower-level variable sizes for different experiments

Experiment	Dataset	Upper-level variable	Lower-level variable
Data denoising	MNIST	59K	1.4M
	CIFAR10	40K	1.2M
	SVHN	72K	1.3M
Few-shot learning	Omniglot	111K	39K
	Mini-Imagenet	3.8M	5K
Data poisoning	Augment 60 poison points (MNIST)	47K	8K
	Clean label attack (ImageNet)	268K	4K

D.1. Synthetic examples

In this experiment, four simple bilevel problems with known optimal solutions are used to check the convergence of different algorithms. The two problems in Fig. 1 are

$$\min_{u,v} \|u\|^2 + \|v\|^2, \text{ s.t. } v = \arg \min_v \|1 - u - v\|^2,$$

and

$$\min_{u,v} \|v\|^2 - \|u - v\|^2, \text{ s.t. } v = \arg \min_v \|u - v\|^2,$$

where $u = [u_1, \dots, u_{10}]^T$, $|u_i| \leq 5$ and $v = [v_1, \dots, v_{10}]^T$, $|v_i| \leq 5$. The optimal solutions are $u_i = v_i = 0.5$, $i = 1, \dots, 10$ for the former and $u_i = v_i = 0$, $i = 1, \dots, 10$ for the latter. Since there

are unique solutions, convergence is measured by the Euclidean distance $\sqrt{\|u - u^*\|^2 + \|v - v^*\|^2}$ of the current iterate (u, v) and the optimal solution (u^*, v^*) .

The two problems in Fig. 2 are

$$\begin{aligned} \min_{u,v} \|u\|^2 + \|v\|^2, \text{ s.t.} \\ v = \arg \min_v (1 - u - v)^T A^T A (1 - u - v) \end{aligned}$$

and

$$\begin{aligned} \min_{u,v} \|v\|^2 - (u - v)^T A^T A (u - v), \text{ s.t.} \\ v = \arg \min_v (u - v)^T A^T A (u - v), \end{aligned}$$

where A is a 5×10 real matrix such that $A^T A$ is rank-deficient, and the domains are the same as before. These problems are ill-conditioned versions of the previous two problems and are more challenging. The optimal solutions to these two example problems are not unique. For the former, the solutions are $u = 0.5 + p$ and $v = 0.5 + p$ for any vector $p \in \text{Null}(A)$. For the latter, $u = p$ and $v = 0$ for any vector $p \in \text{Null}(A)$. Since they are non-unique, convergence is measured by the residual distance $\sqrt{\|P(u - 0.5)\|^2 + \|P(v - 0.5)\|^2}$ for the former and $\sqrt{\|Pu\|^2 + \|v\|^2}$ for the latter, where $P = A^T(AA^T)^{-1}A$ is the orthogonal projection to the row-space of A .

Algorithms used in this experiment are GD, RMD, Approx-Grad, and Penalty. Adam optimizer is used for minimization everywhere except RMD which uses gradient descent for a simpler implementation. The learning rates common to all algorithms are $\sigma_0 = 10^{-3}$ for u -update and $\rho_0 = 10^{-4}$ for v - and p -updates. For Penalty, the values $\gamma_0 = 1$, $\lambda_0 = 10$, and $\epsilon_0 = 1$ are used. For each problem and algorithm, 20 independent trials are performed with random initial locations (u_0, v_0) sampled uniformly in the domain, and random entries of A sampled from independent Gaussian distributions. We test with $T = 1, 5, 10$. Each run was stopped after $K = 40000$ iterations of u -updates.

D.2. Data denoising by importance learning

Following the formulation for data denoising presented in Eq. (3), we associate an importance value (denoted by u_i) with each point in the training data. Our goal is to find the correct values for these u_i 's such that the noisy points are given a lower importance and clean points are given a higher importance value. In our experiments, we allow the importance values to be between 0 and 1. We use the change of variable technique to achieve this. We set $u'_i = 0.5(\tanh(u_i) + 1)$ and since $-1 \leq \tanh(u_i) \leq 1$, u'_i is automatically scaled between 0 and 1. We use a warm start for the bilevel methods (Penalty and ApproxGrad) by

pretraining the network in the lower-level using the validation set and initializing the importance values with the predicted output probability from the pre-trained network. We see an advantage in convergence speed of the bilevel methods with this pretraining. Below we describe the network architectures used for our experiments.

For the experiments on the MNIST dataset, our network consists of a convolution layer with kernel size of 5×5 , 64 filters and ReLU activation, followed by a max pooling layer of size 2×2 and a dropout layer with drop rate of 0.25. This is followed by another convolution layer with 5×5 kernel, 128 filters and ReLU activation followed by similar max pooling and dropout layers. Then we have 2 fully connected layers with ReLU activation of size 512 and 256 respectively, each followed by a dropout layer with a drop rate of 0.5. Lastly, we have a softmax layer with 10 classes. We used the Adam optimizer with a learning rate of 0.00001, batch size of 200 and 100 epochs to report the accuracy of Oracle, Val-Only and Train+Val classifiers. For bilevel training using Penalty we used $K = 100$, $T = 20$, $\sigma_0=3$, $\rho_0=0.00001$, $\gamma_0=0.01$, $\epsilon_0=0.01$, $\lambda_0=0.01$, $\nu_0=0.000001$ as per Alg. 2. For the experiments on the CIFAR10 dataset, our network consists of 3 convolution blocks with filter sizes of 48, 96, and 192. Each convolution block consists of two convolution layers, each with kernel size of 3×3 and ReLU activation. This is followed by a max pooling layer of size 2×2 and a drop out layer with drop rate of 0.25. After these 3 blocks we have 2 dense layers with ReLU activation of size 512 and 256 respectively, each followed by a dropout layer with rate 0.5. Finally we have a softmax layer with 10 classes. This is optimized with the Adam optimizer using a learning rate of 0.001 for 200 epochs with batch size of 200 to report the accuracy of Oracle, Val-Only and Train+Val classifiers. For this experiment we used data augmentation during our training. For the bilevel training using Penalty we used $K = 200$, $T = 20$, $\sigma_0=3$, $\rho_0=0.00001$, $\gamma_0=0.01$, $\epsilon_0=0.01$, $\lambda_0=0.01$, $\nu_0=0.0001$ with mini-batches of size 200. We also use data augmentation for bilevel training. For the experiments on the SVHN dataset, our network consists of 3 blocks each with 2 convolution layers with kernel size of 3×3 and ReLU activation followed by a max pooling and drop out layer (drop rate = 0.3). The two convolution layers of the first block has 32 filters, second block has 64 filters and the last block has 128 filters. This is followed by a dense layer of size 512 with ReLU activation and dropout layer with drop rate = 0.3. Finally we have a softmax layer with 10 classes. This is optimized with the Adam optimizer and learning rate of 0.001 for 100 epochs to report results of Oracle, Val-Only and Train+Val classifiers. The bilevel training uses $K = 100$ and $T = 20$, $\sigma_0=3$, $\rho_0=0.00001$, $\gamma_0=0.01$, $\epsilon_0=0.01$, $\lambda_0=0.01$, $\nu_0=0.0$ with batch-size of 200.

The test accuracy of these models when trained on the entire training data without any label corruption are 99.5% for

MNIST, 86.2% for CIFAR10 and 91.23% for SVHN. For all the experiments with ApproxGrad, we used 20 updates for the lower-level and 20 updates for the linear system and did same number of epochs as for Penalty (i.e. 100 for MNIST and SVHN and 200 for CIFAR), with a mini-batch-size 200.

D.3. Few-shot learning

For these experiments, we used the Omniglot [15] dataset consisting of 20 instances (size 28×28) of 1623 characters from 50 different alphabets and the Mini-ImageNet [32] dataset consisting of 60000 images (size 84×84) from 100 different classes of the ImageNet [7] dataset. For the experiments on the Omniglot dataset we used a network with 4 convolution layers to learn the common representation for the tasks. The first three layers of the network have 64 filters, batch normalization, ReLU activation and a 2×2 max-pooling. The final layer is same as the previous ones with the exception that it does not have any activation function. The final representation size is 64. For the Mini-ImageNet experiments we used a residual network with 4 residual blocks consisting of 64, 96, 128 and 256 filters followed by a 1×1 convolution block with 2048 filters, average pooling and finally a 1×1 convolution block with 512 filters. Each residual block consists of 3 blocks of 1×1 convolution, batch normalization, leaky ReLU with leak = 0.1, before the residual connection. The last 512 convolution block does not have any activation function. The final representation size is 512. Similar architectures have been used by [11] in their work with a difference that we don't use any activation function in the last layers for our experiments and have a slightly bigger representation size for Mini-Imagenet (512 vs. 384). For both the datasets, the lower-level problem is a softmax regression with a difference that we normalize the dot product of the input representation and the weights with the l_2 -norm of the weights and the l_2 norm of the input representation. For N way classification, the dimension of the weights in the lower-level are $64 \times N$ for Omniglot and $512 \times N$ for Mini-ImageNet. For our Omniglot experiments we use a meta-batch-size 30 for 5-way and 20-way classification and a meta-batch-size of 2 for 5-way classification with Mini-ImageNet. We use $T = 20$ iterations for the lower-level in all experiments. The hyper-parameters used for Penalty are $\sigma_0=0.001$, $\rho_0=0.001$, $\gamma_0=0.01$, $\epsilon_0=0.01$, $\lambda_0=0.01$, $\nu_0=0.0001$.

D.4. Training-data poisoning

For this experiment, we used l_2 -regularized logistic regression implemented as a single layer neural network with the cross entropy loss and a weight regularization term with a coefficient of 0.05. The model is trained for 10000 epochs using the Adam optimizer with learning rate of 0.001 for training with and without poisoned data. We pre-train the lower-level with clean training data for 5000 epochs with

the Adam optimizer and learning rate 0.001 before starting bilevel training. For untargeted attacks, we optimized Penalty is with $K = 5000$, $T = 20$, $\sigma_0=0.1$, $\rho_0 = 0.001$, $\gamma_0=10$, $\epsilon_0=1$, $\lambda_0=100$, $\nu_0=0.0$. The test accuracy of this model trained on clean data untargeted case is 87%. For targeted attack, Penalty is optimized with $K = 5000$, $T = 20$, $\sigma_0=0.1$, $\rho_0 = 0.001$, $\gamma_0=10$, $\epsilon_0=1$, $\lambda_0=1$, $\nu_0=0.0$.

D.4.1. CLEAN LABEL ATTACK

The goal of clean label attack is to find poisoning points which appear to have correct labels, when visually inspected, but a classifier trained on original training data augmented with these poisoned points, leads to misclassification of specific target images. We use the dog vs. fish image dataset as used by [14], consisting of 900 training and 300 testing examples from each of the two classes. The size of the images in the dataset is 299×299 with pixel values scaled between -1 and 1. Following the setting in Sec. 5.2 of [14], we use InceptionV3 network, with weights pre-trained on ImageNet, for our representation map (2048 dimensional) and train a fully connected layer on top of this representation to classify dogs and fishes. For a given target image t from the test set, a base image b whose representation is the closest to the representation of the target image and has the opposite label is chosen from the training set. Inspired by [30], we have the following bilevel formulation for this attack:

$$\begin{aligned} \arg \min_u L_t(u, w) + \alpha \|r(t) - r(u)\|_2^2 + \beta \|b - u\|_2^2 \\ \text{s.t. } w = \arg \min_w L_{X \cup \{u\}}(w), \end{aligned} \quad (10)$$

where L_t is the loss of the given target image associated with the opposite label, and $r(\cdot)$ is the 2048-dimensional representation obtained from the InceptionV3 model. The second term in the upper-level penalizes the difference between the representations of the poisoned image and the target image t , and the third term in the upper-level forces the poisoned image to be close to the base image b in the input space ensuring that the poisoned image appears similar to the base image to avert detection. α and β control the relative importance of these terms. To test the performance of the attack we retrain only the fully connected layer with original training data augmented with the poisoned point obtained from Penalty. Attack is considered successful if the target point, which is correctly classified before poisoning (there are 590 such test images out of 600), is misclassified after retraining on the augmented training dataset. We generate poisoned point for each target image one by one. The attack success of Penalty using just a single poisoned point per target image is 100%. For comparison, the attack success with using a single poisoned point by [14] and [30] are 57% and 100% respectively. As shown in Fig. 7 of Appendix D.4, our poisoned points obtained from solving Eq. (10) are indistinguishable from the original base points



Figure 5. Untargeted data poisoning attack on MNIST. The top row shows the learned poisoned image using Penalty, starting from the images in the bottom row as initial poisoned images. The column number represents the fixed label of the image, i.e. the label of the images in first column is digit 0, the label of the second column is digit 1, etc.



Figure 6. Targeted data poisoning attack on MNIST. The top row shows the learned poisoned images using Penalty, starting from the images in the bottom row as initial poisoned images. The images in the first 5 columns have the fixed label of digit 3, and in the next 5 columns are images with the fixed label of digit 8.

but still misclassify the target point during retraining.

Experiment Details: We use the InceptionV3 model with weights pre-trained on ImageNet. We train a fully connected layer on top of these pre-trained features using the RMSProp optimizer and a learning rate of 0.001 optimized for 2000 epochs. The test accuracy obtained with training on clean training data is 98.33. We repeat the exact same procedure as training during evaluation and train with softmax layer using the training data augmented with the poisoned point obtained from Penalty, for measuring attack success. The Penalty method is optimized with $K = 600$, $T = 10$, $\sigma_0=0.01$, $\rho_0 = 0.001$, $\gamma_0=1$, $\epsilon_0=1$, $\lambda_0=1$.



Figure 7. Clean label poisoning attack on dog-fish dataset. The top row shows the target instances from the test set, the second row shows the base instances from the training set used to initialize the poisoned images and the last row shows the poisoned instances obtained from Penalty. Notice that poisoned images (third row) are visually indistinguishable from the base images (second row) and can evade visual detection.